

Design of a 1×2 CPW Fractal Antenna Array on Plexiglas Substrate with Defected Ground Plane for Telecommunication Applications

Chiraz Ben Nsir

Department of Physics
University of Tunis El Manar
Tunis, Tunisia
chiraz.bennsir@fst.utm.tn

Chokri Boussetta

Department of Physics
University of Tunis El Manar
Tunis, Tunisia
chboussetta2020@gmail.com

Jean-Marc Ribero

Department of Electronics
University of Nice Sophia Antipolis
Nice, France
jean-marc.ribero@unice.fr

Ali Gharsallah

Department of Physics
University of Tunis El Manar
Tunis, Tunisia
ali.gharsallah@fst.utm.tn

Abstract—In this paper, a fractal antenna array for telecommunication applications is presented. The proposed antenna array is realized on a Plexiglas substrate, has 1×2 radiating elements, and dimensions of $170\text{mm} \times 105\text{mm}$. The antenna array is composed of two Koch Snowflake patches and is fed by a Coplanar Waveguide (CPW) transmission line. Radiating elements and the ground plane are printed on the top side of the substrate. Defected Ground Structure (DGS) technique is employed to enhance the bandwidth and improve the impedance matching. The proposed antenna array operates at two frequency bands, 1.08-1.32GHz covering the GPS band and 1.7-3.7GHz covering the GSM 1800/1900, UTMS, Bluetooth, LTE, and WiMAX bands. In addition, the antenna has a good performance with efficiency and peak gain of 82% and 6.3dB respectively. These characteristics allow the antenna to be an attractive candidate for telecommunication systems. Design and analysis of different structures were carried out with Ansys HFSS.

Keywords—fractal antenna array; DGS; CPW; wideband

I. INTRODUCTION

The advance in the telecommunication systems has increased significantly during the last years. Many research efforts have been focused to the integration of antennas into telecommunication systems because of their ease of implementation and their low cost. Moreover, the use of glass in the construction of buildings has increased. Therefore, the exploitation of these surfaces for the implementation of antennas is imposed. Antennas with small size and broadband behavior, operating in telecommunication frequency bands are highly recommended. Several techniques are used to achieve bandwidth enhancement. For instance, adding stubs [1] to the radiating element can improve bandwidth. Incorporation of slots on different parts of the antenna is another technique to

obtain broadband features [2-4]. The Coplanar Waveguide (CPW) is the most popular feeding structure utilized for multiband and wideband applications. Several studies prioritize the use of CPW over other excitation techniques, such as the microstrip line, due to features such as the ease of manufacturing, low cost, and wide bandwidth. Many antenna structures that include CPW feed-line have been studied and reported [5-12]. Consequently, the rapid demand of this kind of excitation keeps increasing. Among the techniques used to enhance bandwidth using CPW feed, is the optimization of either the distance between the ground plane and the radiator [13] or the distance between the feed line and the ground plane [14]. Thus, due to the features mentioned above, the CPW is chosen as the feed for the proposed antenna.

Antenna miniaturization is as an interesting topic as the broad-band antenna is. Reducing the size of the antennas can decrease their performance in terms of bandwidth, pattern stability, and efficiency. Thus, many studies have been focused to found an acceptable compromise between antenna size and its features. Antenna miniaturization techniques can affect either the geometry of the antennas by modifying their shapes or their electrical and magnetic characteristics. In [15], an overview has been presented to describe the most important techniques used for antenna miniaturization and the exploitation of these techniques for achieving wideband applications. Fractal geometry [16-17] is one of the most attractive techniques used for antenna design. The main properties of fractal antennas are their self-similarity and space-filling. Self-similarity shows multi-band and wide-band capabilities, while, with space-filling, the perimeter of the antenna can increase without changing the overall size. This property has been used for size reduction. Therefore, the use of fractal structures is a good technique for achieving miniaturized

Corresponding author: Chokri Boussetta

antennas [18]. Recently, numerous fractal geometries have been used to design antennas with compact size and wide bandwidth [19-22]. For instance, a microstrip patch antenna composed with Minkowski island and crossbar fractal layers operating from 4.1 to 19.4GHz for broadband applications has been proposed in [19]. The antenna presented in [20] has been designed using mushroom fractal geometry to achieve wide bandwidth. A novel broadband circular antenna with fractal elements was presented in [21]. Compactness and bandwidth enhancement were obtained in [22] using Koch geometry with the incorporation of modified ground plane and meandering slits, to design a wearable fractal antenna for the ISM band.

From the literature review, it was proved that using fractal geometry with the combination of various techniques can improve the antenna's performance. The proposed antenna array can be printed on a Plexiglas window. Thus, if the ground plane is placed on the bottom side of the Plexiglas substrate (i.e. the outside of the window), there will be a risk of degradation of the antenna performance by external factors such as rain, wind, and pollution. Therefore, the most beneficial is to put the total structure on the top side of the Plexiglas substrate (i.e. the inside of the window). As a result, the most appropriate technique is the use of CPW as feed. In this manner, the radiating elements, feed line, and ground planes will be printed on the same side of the substrate. In addition, the CPW feed insures wider impedance bandwidth, simple structure, low cost, and less radiation loss. The Koch structure [18] has shown the best results compared to the traditional simple patches in terms of efficiency, gain, miniaturization, and multiband and broadband behavior. Also, DGS technique is applied to further improve the bandwidth.

In this paper, a 1x2 fractal antenna array is proposed for telecommunication applications. The proposed antenna is composed by two Koch snowflake fractal patches and CPW is used for feeding. Modified ground plane is employed to enhance bandwidth and improve the impedance matching. Details of the antenna array, simulation results, and measurement are analyzed in the following sections.

II. THE SINGLE FRACTAL ANTENNA DESIGN

A. Koch Snowflake Geometry

The procedure shown in Figure 1 is adopted to generate the Koch snowflake fractal geometry. The Koch structure starts with an equilateral triangle with S being the side of the triangle. In order to obtain the first iteration, an equilateral triangle, which has a side S/3, is placed in the middle of each side of the basic triangle. Therefore, six equilateral triangles appear which have S/3 as side. In the same way, iteration 2 is constituted. In this case, an equilateral triangle, which has a side of S/9, is placed in the middle of each side of generated triangles. After n iterations, the side length of the produced triangles is S/3^n. As the number of iterations increases, the surface of the Koch snowflake tends towards a finite value while its perimeter tends to infinity. The perimeter of the Koch Snowflake after n iterations is given by:

$$P_n = 3 \left(\frac{4}{3}\right)^n S \quad (1)$$

The area of the Koch snowflake converges to:

$$A = \frac{2\sqrt{3}}{5} s^2 \quad (2)$$

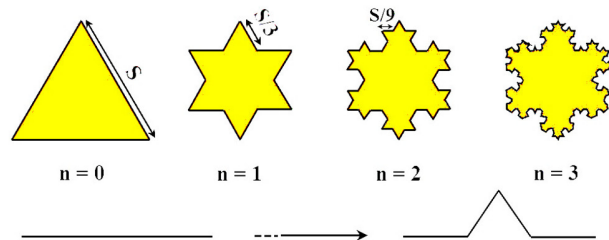


Fig. 1. The Koch snowflake Iterations.

B. Koch Snowflake Geometry

The configuration of the single Koch snowflake antenna for dual-band operation is shown in Figure 2. This antenna is implemented on Plexiglas substrate with dielectric constant ε_r=2.6, thickness h=4mm and dimensions LxW=70x60mm². The radiating element is fed by a CPW transmission line which has a width of W_f=5mm, length L_f=25.6mm, and is separated from the ground plane with a gap distance of G=0.238mm. The width of the feed and the distance of the gap have been optimized to provide 50Ω characteristic impedance.

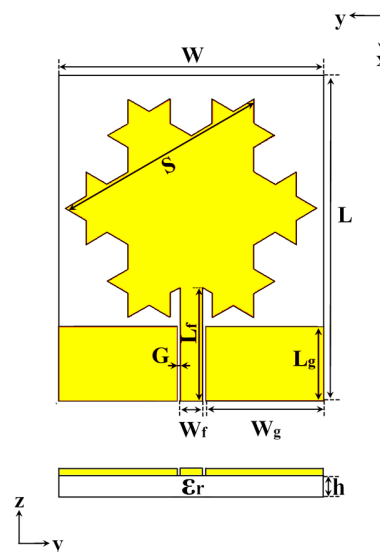


Fig. 2. Single Koch snowflake antenna configuration.

Initially, this antenna is composed by an equilateral triangular patch having S as side length and two limited ground planes which are placed symmetrically with respect to the CPW line. Then, the Koch snowflake geometry is obtained by adding two Koch iterations as shown in Figure 2. The optimized dimensions for this fractal antenna element are listed in Table I. The resonance frequency [23] of such an antenna is given by:

$$f_r = \frac{2c}{3s_e \sqrt{\epsilon_r}} \quad (3)$$

$$S_e = S \left[1 + 2.199 \frac{h}{s} - 12.853 \frac{h}{s\sqrt{\epsilon_r}} + 16.436 \frac{h}{s\epsilon_r} + 6.182 \left(\frac{h}{s} \right)^2 - 9.802 \frac{1}{\sqrt{\epsilon_r}} \left(\frac{h}{s} \right)^2 \right] \quad (4)$$

where f_r is the resonant frequency, c the speed of light, ϵ_r the relative permittivity of the substrate, h the height of the substrate, S the patch side length, and S_e the effective patch side length.

TABLE I. OPTIMIZED SINGLE ANTENNA PARAMETERS

Parameters	Value (mm)	Parameters	Value (mm)
L	70	L_f	25.6
W	60	W_g	27.262
S	49.3	L_g	17.5
W_f	5	G	0.238

C. Results and Discussion

After fixing the CPW parameters and the side length S to 49.3mm, the proposed single Koch snowflake antenna is simulated. Figure 3 shows the reflection coefficient S_{11} of the simulated antenna. It can be observed that the proposed antenna covers two bands, 0.90-2.55GHz and 3.41-3.54GHz. The use of fractal geometry increases the perimeter length of the radiating element by increasing its electrical path without changing the total volume of the antenna. This method improves the antenna bandwidth and leads to reduced size.

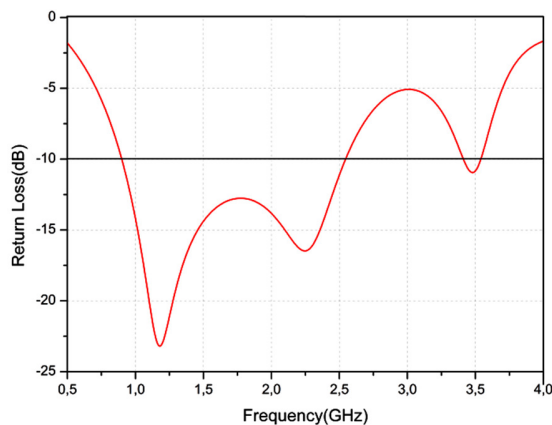


Fig. 3. Simulated return loss of the single antenna.

Figure 4 shows the radiation pattern of the proposed single antenna at three frequencies, 1.8, 2.1, and 2.4GHz selected from the operating band, 0.90-2.55GHz. From the Figure, it is clear that the simulated radiation patterns are bidirectional in the E-plane and H-plane at all frequencies.

In this section, the basic element Koch snowflake fractal antenna was designed and optimized. This antenna attains good results in terms of bandwidth, return loss, and gain. In the following section, the previously developed single antenna is duplicated to form a fractal antenna array which is subsequently optimized to enhance the gain and improve the bandwidth in order to be suitable for integration in telecommunication systems.

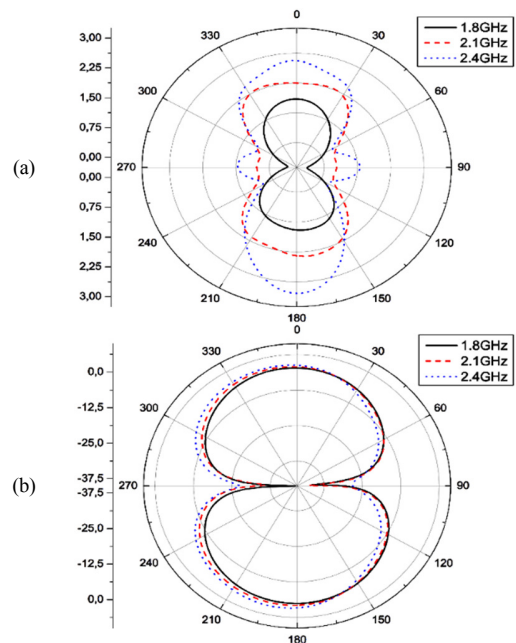


Fig. 4. Simulated radiation patterns of the single antenna at 1.8, 2.1, 2.4GHz: (a) E-plane, (b) H-plane.

III. THE PROPOSED ANTENNA ARRAY DESIGN

The proposed 1×2 fractal antenna array is shown in Figure 5. The two Koch snowflake elements are identical to the basic single antenna previously reported. This antenna array is printed on the same substrate. The dimensions of the substrate are $170 \times 105 \text{mm}^2$. $D = 91 \text{mm}$ is the distance between the two fractal elements. The optimized parameters of the 1×2 antenna array are summarized in Table II. The modification in the ground-plane is used for the antenna array to achieve wider bandwidth with good impedance matching. The proposed antenna array is excited by the T-junction power divider [24] which has an input impedance of 50Ω .

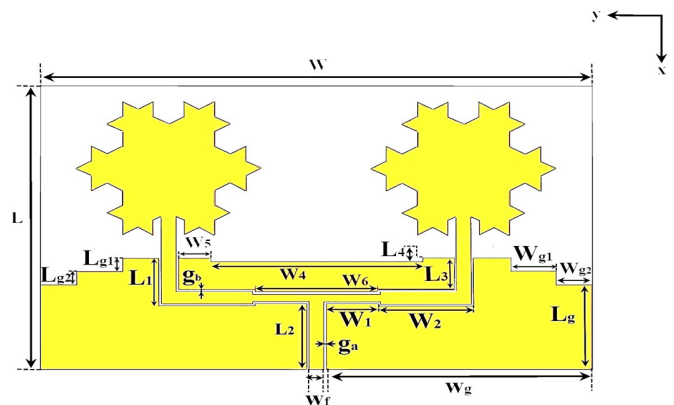


Fig. 5. Configuration of the proposed antenna array.

Figure 6 shows the proposed power divider. $Z_a = 50 \Omega$ and $Z_b = 70.7 \Omega$ are the CPW line impedances used for feeding the antenna array. The width of the power divider as well as the gap between the ground plane and the divider play a crucial role for the determination of the characteristic impedances.

The gaps ($g_a = 0.238\text{mm}$ and $g_b = 0.612\text{ mm}$) and the widths ($W_f = 5\text{mm}$ and $W_{f1} = 3\text{mm}$) are used to obtain Z_a and Z_b . Equation (5) [25] is applied to determine these two impedances:

$$Z = \frac{30\pi}{\sqrt{\epsilon_e}} \frac{K(k'_0)}{K(k_0)} \quad (5)$$

$$\epsilon_e = 1 + \frac{(\epsilon_r - 1)}{2} \left(\frac{K(k'_0)}{K(k_0)} \right) \left(\frac{K(k_1)}{K(k'_1)} \right) \quad (6)$$

where ϵ_e is the effective dielectric constant, K is the complete elliptic integral of the first kind, $k' = \sqrt{1 - k^2}$, and (k_0, k_1) are given as:

$$k_0 = \frac{W_f}{W_f + 2g} \quad (7)$$

$$k_1 = \frac{\sinh(\pi W_f / 4h)}{\sinh(\pi [W_f + 2g] / 4h)} \quad (8)$$

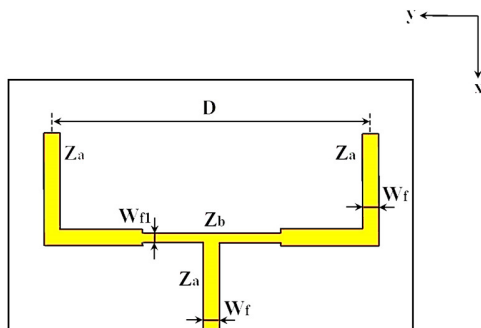


Fig. 6. The proposed power divider.

TABLE II. OPTIMIZED ANTENNA ARRAY PARAMETERS

Parameter	Value (mm)	Parameter	Value (mm)	Parameter	Value (mm)
W	170	W_g	82.262	L_f	25.6
W_1	16.449	W_{g1}	11	L_{f1}	25
W_2	29.051	W_{g2}	14	L_g	13.48
W_3	23.575	W_{g3}	25	L_{g1}	5.01
W_4	65	L	105	L_{g2}	5.01
W_5	10.262	L_1	17.738	s	49.3
W_6	38.374	L_2	24.388	D	91
W_f	5	L_3	12.262	g_a	0.238
W_{f1}	3	L_4	1.4	g_b	0.612

D. Design Procedure

The developed antenna array is carried out in four steps:

- Step-1: A fractal antenna array including a rectangular ground plane with a CPW power divider to feed the two radiating elements is designed.
- Step-2 and step-3: To enhance the impedance bandwidth and to obtain good impedance matching, the ground plane is modified to form a staircase on its upper edges. Two pairs of steps are used to form the staircase shape. The first pair is cut out from the ground plane, which has a size $L_{g1} \times W_{g3}$ of $5.01 \times 25\text{mm}^2$. Then, the second pair is cut out from the ground plane, which has a size $L_{g2} \times W_{g2}$ of $5.01 \times 14\text{mm}^2$. The relation between W_{g1} , W_{g2} , and W_{g3} is: $W_{g3} = W_{g1} + W_{g2}$.

- Step-4: Finally, the proposed antenna array is obtained by etching a rectangular slot, with a size $L_4 \times W_4$ of $1.4 \times 65\text{mm}^2$, in the rectangular ground plane placed between the two radiating elements in order to achieve the desired band.

E. Simulation Results and Parametric Study

Figure 7 shows the simulated S_{11} of the proposed fractal antenna array with and without stepped ground plane. According to the results, Koch snowflake fractal geometry contributes to the appearance of multi-band behavior by increasing the electrical length of the radiating elements. Moreover, stepped ground plane is used to improve the impedance matching. Indeed, the steps in the ground plane create close resonances. The combination of these resonances generates a wide bandwidth. In addition, by adding a rectangular slot in the ground plane, a new path is added for the current thus helping to further increase the bandwidth. Hence, the use of fractal geometry and DGS allows the designed antenna to achieve two operating bands, 1.13-1.39GHz covering the GPS band and 1.79-3.66GHz covering GSM 1800/1900, UTMS, Bluetooth, LTE, and WiMAX bands.

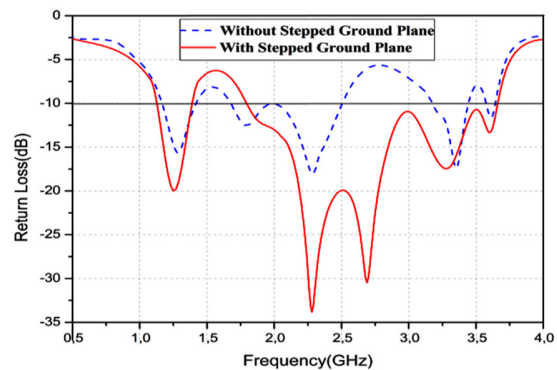


Fig. 7. Simulated return loss of the antenna array with and without stepped ground plane.

Three parameters are studied in order to evaluate their effects on the antenna and subsequently to choose the optimum values which improve the antenna performance.

1) Effect of length L_{g1}

L_{g1} is the length of the first step introduced in the ground plane. This parameter varies from 3.01mm to 6.01mm. The effect of varying L_{g1} on the return loss is shown in Figure 8. It is noticed that for different values of L_{g1} there are practically three frequency bands. By varying the parameter L_{g1} the impedance matching of the second band improves. Indeed, for $L_{g1} = 3.01\text{mm}$, the second band has an operating band from 1.73 to 2.94GHz and the return loss does not exceed -25dB. Thus, by increasing L_{g1} , the impedance matching enhances significantly in this band and for the optimum value $L_{g1} = 5.01\text{mm}$, the appearance of two resonant frequencies of 2.32 and 2.63GHz with an important value of return loss is observed. This result proves that L_{g1} has an effect on impedance matching enhancement.

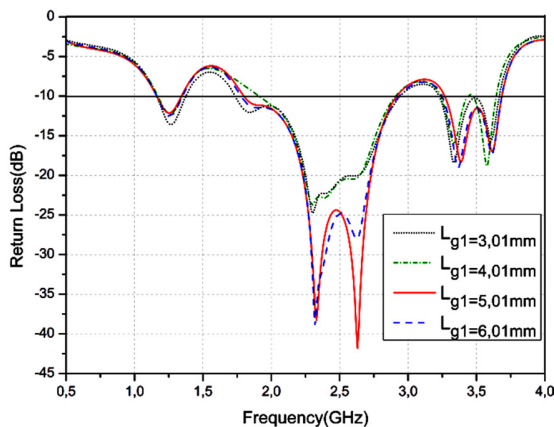


Fig. 8. Simulated return loss for different values of L_{g1} .

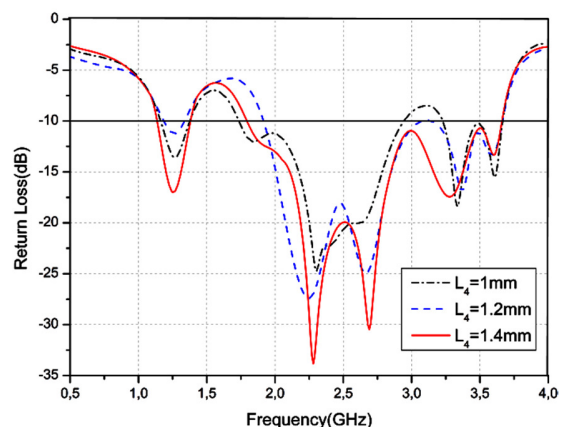


Fig. 10. Simulated return loss for different values of L_4 .

2) Effect of width W_{g2}

The second parameter W_{g2} is the width of the second step of the staircase shaped modified ground plane and is varied from 9mm to 12mm as shown in Figure 9. It is observed from the result that by increasing the width W_{g2} , the upper cut-off frequency of the second band shifts toward the upper frequencies and starts to merge with the adjacent third band. A better result is obtained for $W_{g2} = 11$ mm. It is observed from the Figure that the impedance bandwidth ranges from 1.8 to 3.05GHz for the second band, while it ranges from 3.18 to 3.69GHz for the third band with a good return loss at both frequency bands. The obtained result proves that the parameter W_{g2} affects the impedance bandwidth of the proposed antenna and leads to better performance.

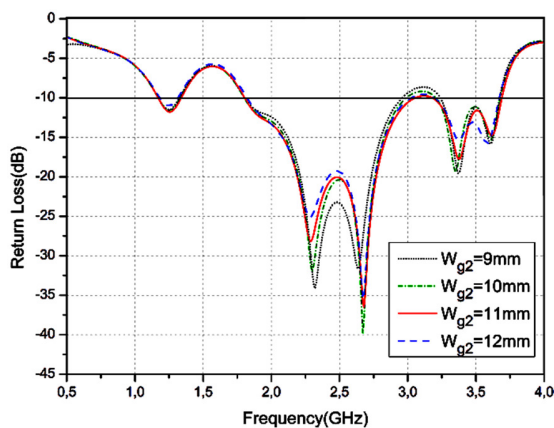


Fig. 9. Simulated return loss S_{11} for different values of W_{g2} .

3) Effect of Length L_4

By increasing L_4 from 1mm to 1.4mm as shown in Figure 10, the second and third frequency bands are combined, for $L_4 = 1.4$ mm, to form wideband ranges from 1.79 to 3.66GHz with a great impedance matching. However, the first frequency band remains almost in the same frequency range of 1.13 to 1.38GHz with a resonant frequency of 1.25GHz and with a return loss of -17dB. This result shows the effect of varying L_4 which leads to bandwidth improvement of the fractal antenna array and consequently covering the desired dual band.

IV. FABRICATION AND MEASURED RESULTS

To validate the simulated results carried out by Ansys HFSS, the proposed antenna was fabricated and tested. Figure 11 shows the prototype of the fabricated antenna array.



Fig. 11. The fabricated antenna array.

Figure 12 shows the simulated and measured return loss. A good agreement between the two curves is observed. The measured S_{11} is below -10dB from 1.7 to 3.7GHz. A small difference between simulation and measurement can be explained by manufacturing defects.

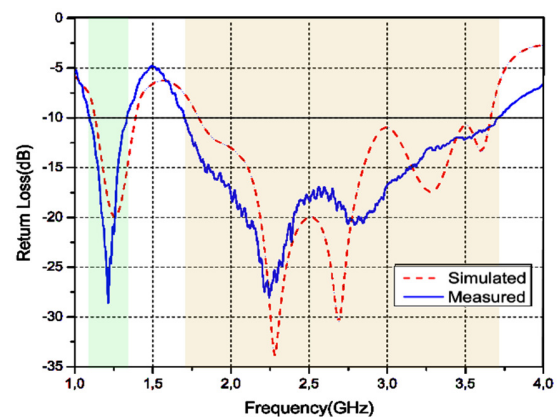


Fig. 12. Simulated and measured return loss of the proposed antenna array.

The radiation patterns of the proposed antenna array were measured in an anechoic chamber. Figure 13 shows the measured radiation patterns at the frequencies 1.8, 2.1, 2.4, and 2.6GHz in the E-plane and the H-plane. From these results, it is clear that the radiation pattern is bi-directional at all frequencies. The measured peak gain and total efficiency are shown in Figure 14. The peak gain is between 5.3dB and 6.3dB from 1.7 to 2.1GHz and between 6dB and 6.25dB from 2.3 to 2.7GHz. The minimum value of peak gain is 3.43dB at 2.16GHz. In addition, total efficiency is between 44% and 82% over the band 1.7-2.7GHz.

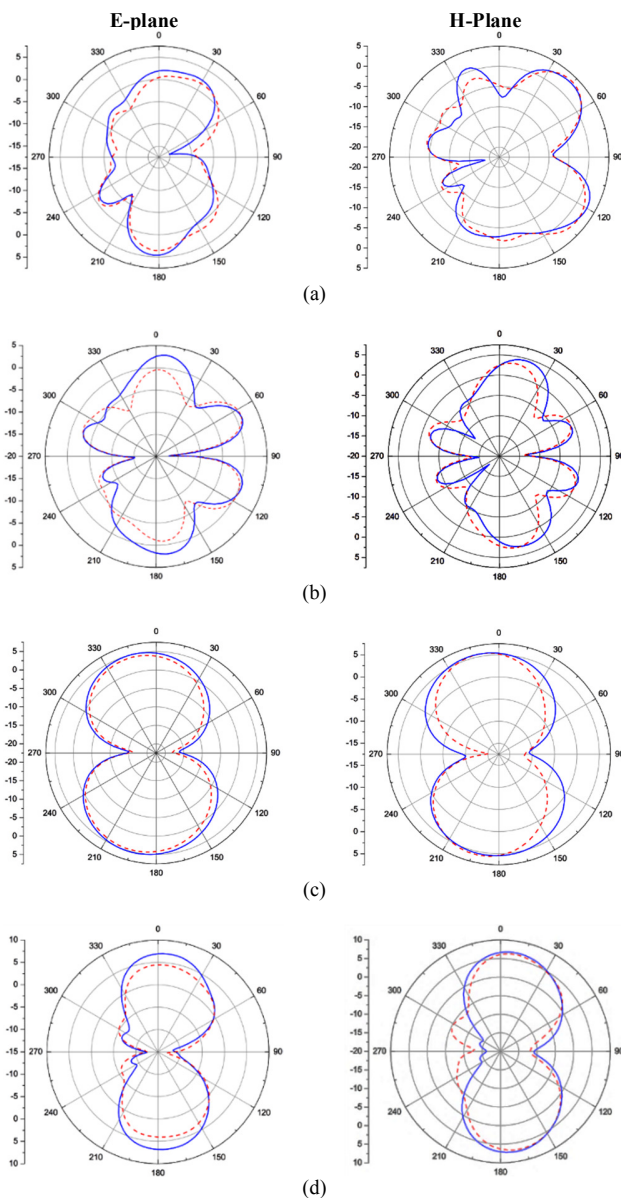


Fig. 13. Measured (solid line) and simulated (dashed line) radiation patterns of the proposed antenna in the E-plane and H-plane at: (a) 1.8GHz, (b) 2.1GHz, (c) 2.4GHz, and (d) 2.6GHz.

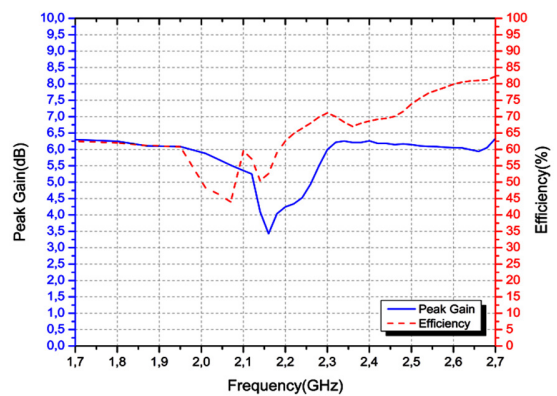


Fig. 14. Measured antenna peak gain and efficiency.

V. COMPARATIVE STUDY

Table III lists a comparison of the performance of the proposed Koch snowflake fractal antenna array with other, reported antenna arrays. The proposed antenna has a higher gain than those in [26-30]. In addition, the incorporation of Koch geometry, DGS, and CPW feed in the same structure has allowed the proposed antenna to obtain the widest impedance bandwidth compared to those in [27-30]. Therefore, these features make this antenna more advantageous for telecommunication systems than the previously reported antennas.

TABLE I. COMPARISON OF THE PROPOSED WITH OTHER ANTENNA ARRAYS

Ref.	Array type	Feed method	Operating bands/ frequency bands (GHz)	BW (%)	Max gain
[26]	Octagonal fractal antenna array with DGS	Microstrip line feeding	2.3-14	140.64	<3.5 at lower frequencies
[27]	Hexagonal fractal antenna array	Coaxial feeding	1.3, 1.6, 2.4	2.76, 5.625, 4.33	Not given
[28]	Rectangular antenna array with DGS	Microstrip line feeding	2.2	5.45	4.14
[29]	Hexagonal fractal antenna array with DGS	Microstrip line feeding	2.6, 3.5, 5.7	15.38, 8.57, 4.38	4.2, 3.8, 3.6
[30]	E-shaped antenna array	Microstrip line feeding	2.45	3.67	2.48
Proposed	Koch fractal antenna array with DGS	CPW feeding	1.08-1.32, 1.7-3.7	19.83, 79.68	6.3

VI. CONCLUSION

A Koch snowflake fractal antenna array with CPW-fed printed on transparent substrate has been studied. The antenna achieved wideband characteristics and provided good performance in terms of return loss, radiation pattern, gain, and efficiency. The parametric study on the ground plane, which was modified using the DGS technique, contributed to the bandwidth enhancement of the proposed antenna. A good

accordance was acquired between the simulated and the experimental results. The designed antenna operates in two bands, 1.08-1.32GHz for GPS applications and 1.7-3.7GHz for GSM, UTMS, Bluetooth, LTE, and WIMAX applications. The obtained results make the antenna array suitable for telecommunication applications.

REFERENCES

- [1] K. Li, T. Dong, and Z. Xia, "Wideband Printed Wide-Slot Antenna with Fork-Shaped Stub," *Electronics*, vol. 8, no. 3, Mar. 2019, Art. no. 347, <https://doi.org/10.3390/electronics8030347>.
- [2] M. M. Nahas and M. Nahas, "Bandwidth and Efficiency Enhancement of Rectangular Patch Antenna for SHF Applications," *Engineering, Technology & Applied Science Research*, vol. 9, no. 6, pp. 4962-4967, Dec. 2019, <https://doi.org/10.48084/etasr.3014>.
- [3] M. S. Karoui, N. Ghariani, M. Lahiani, and H. Ghariani, "Bandwidth Enhancement of a Bell-shaped UWB Antenna for Indoor Localization Systems," *Engineering, Technology & Applied Science Research*, vol. 11, no. 1, pp. 6691-6695, Feb. 2021, <https://doi.org/10.48084/etasr.3975>.
- [4] A. Birwal, S. Singh, B. K. Kanaujia, and S. Kumar, "Broadband CPW-fed circularly polarized antenna for IoT-based navigation system," *International Journal of Microwave and Wireless Technologies*, vol. 11, no. 8, pp. 835-843, Oct. 2019, <https://doi.org/10.1017/S1759078719000461>.
- [5] F. Faisal, Y. Amin, Y. Cho, and H. Yoo, "Compact and Flexible Novel Wideband Flower-Shaped CPW-Fed Antennas for High Data Wireless Applications," *IEEE Transactions on Antennas and Propagation*, vol. 67, no. 6, pp. 4184-4188, Jun. 2019, <https://doi.org/10.1109/TAP.2019.2911195>.
- [6] M. A. Riheen, T. Nguyen, T. K. Saha, T. Karacolak, and P. K. Sekhar, "CPW Fed Wideband Bowtie Slot Antenna on PET Substrate," *Progress In Electromagnetics Research C*, vol. 101, pp. 147-158, 2020, <https://doi.org/10.2528/PIERC20031402>.
- [7] P. Sharma and P. P. Bhattacharya, "Design and Development of a New Wideband CPW Fed Patch Antenna for Wireless Communication," *EAI Endorsed Transactions on Internet of Things*, vol. 5, no. 17, Jan. 2019, Art. no. e4, <https://doi.org/10.4108/eai.31-10-2018.162734>.
- [8] M. Karthikeyan, R. Sitharthan, T. Ali, and B. Roy, "Compact multiband CPW fed monopole antenna with square ring and T-shaped strips," *Microwave and Optical Technology Letters*, vol. 62, no. 2, pp. 926-932, 2019, <https://doi.org/10.1002/mop.32106>.
- [9] F. B. Ghenaya, R. Ghayoula, and A. Gharsallah, "A Novel Linear Array Antenna Based on UWB Slot Antenna," *American Journal of Applied Sciences*, vol. 13, no. 3, pp. 290-298, 2016.
- [10] S. Patil, A. K. Pandey, and V. K. Pandey, "A Compact, Wideband, Dual Polarized CPW-Fed Asymmetric Slot Antenna for Wireless Systems," *Journal of Microwaves, Optoelectronics and Electromagnetic Applications*, vol. 19, pp. 343-355, Sep. 2020, <https://doi.org/10.1590/2179-10742020v19i3827>.
- [11] B. Jmai, S. Gahgouh, and A. Gharsallah, "A Novel Reconfigurable MMIC Antenna with RFMEMS Resonator for Radar Application at K and Ka Bands," *International Journal of Advanced Computer Science and Applications*, vol. 8, no. 5, pp. 468-473, 2017.
- [12] Y. I. Abdulkarim *et al.*, "Design of a Broadband Coplanar Waveguide-Fed Antenna Incorporating Organic Solar Cells with 100% Insolation for Ku Band Satellite Communication," *Materials*, vol. 13, no. 1, Jan. 2020, Art. no. 142, <https://doi.org/10.3390/ma13010142>.
- [13] S. Hu, Y. Wu, Y. Zhang, and H. Zhou, "Design of a CPW-Fed Ultra Wide Band Antenna," *Open Journal of Antennas and Propagation*, vol. 1, no. 2, pp. 18-22, Sep. 2013, <https://doi.org/10.4236/ojapr.2013.12005>.
- [14] R. Kumar and S. Gaikwad, "On the design of nano-arm fractal antenna for UWB wireless applications," *Journal of Microwaves, Optoelectronics and Electromagnetic Applications*, vol. 12, pp. 158-171, Jun. 2013, <https://doi.org/10.1590/S2179-10742013000100013>.
- [15] M. Fallahpour and R. Zoughi, "Antenna Miniaturization Techniques: A Review of Topology- and Material-Based Methods," *IEEE Antennas and Propagation Magazine*, vol. 60, no. 1, pp. 38-50, Feb. 2018, <https://doi.org/10.1109/MAP.2017.2774138>.
- [16] A. Bunde and S. Havlin, "Fractal Geometry, A Brief Introduction to," in *Mathematics of Complexity and Dynamical Systems*, New York, NY, USA: Springer, 2009, pp. 409-428.
- [17] M. Nurujjaman, A. Hossain, and D. P. Ahmed, "A Review of Fractals Properties: Mathematical Approach," *Science Journal of Applied Mathematics and Statistics*, vol. 5, no. 3, pp. 98-105, May 2017, <https://doi.org/10.11648/j.sjams.20170503.11>.
- [18] A. Reha, A. El Amri, O. Benhammouch, and A. Oulad Said, "Fractal Antennas : A Novel Miniaturization Technique for wireless Networks," *Transactions on Networks and Communications*, vol. 2, no. 5, pp. 165-193, Oct. 2014, <https://doi.org/10.14738/tnc.25.566>.
- [19] R. Kubacki, M. Czyżewski, and D. Laskowski, "Minkowski Island and Crossbar Fractal Microstrip Antennas for Broadband Applications," *Applied Sciences*, vol. 8, no. 3, Mar. 2018, Art. no. 334, <https://doi.org/10.3390/app8030334>.
- [20] S. Nelaturi and N. V. S. N. Sarma, "Compact Wideband Microstrip Patch Antenna based on High Impedance Surface," *Engineering, Technology & Applied Science Research*, vol. 8, no. 4, pp. 3149-3152, Aug. 2018, <https://doi.org/10.48084/etasr.1971>.
- [21] A. Dastranj, F. Ranjbar, and M. Bornapour, "A New Compact Circular Shape Fractal Antenna for Broadband Wireless Communication Applications," *Progress In Electromagnetics Research C*, vol. 93, pp. 19-28, 2019, <https://doi.org/10.2528/PIERC19031001>.
- [22] A. Arif, M. Zubair, M. Ali, M. U. Khan, and M. Q. Mehmood, "A Compact, Low-Profile Fractal Antenna for Wearable On-Body WBAN Applications," *IEEE Antennas and Wireless Propagation Letters*, vol. 18, no. 5, pp. 981-985, May 2019, <https://doi.org/10.1109/LAWP.2019.2906829>.
- [23] M. Dadel, K. P. Tiwary, and S. Srivastava, "Log periodic triangular patch array antenna with gap coupled feed," in *International Conference on Signal Processing and Communication*, Noida, India, Mar. 2015, pp. 99-104, <https://doi.org/10.1109/ICSPCom.2015.7150628>.
- [24] Y. A. Rayisiwi and T. Hariyadi, "Design of A 1:12 Power Divider at 5 GHz for Ground Surveillance Radar Application," *IOP Conference Series: Materials Science and Engineering*, vol. 384, Jul. 2018, Art. no. 012053, <https://doi.org/10.1088/1757-899X/384/1/012053>.
- [25] R. N. Simons, *Coplanar Waveguide Circuits, Components, and Systems*. New York, NY, USA: Wiley, 2001.
- [26] S. Tripathi, A. Mohan, and S. Yadav, "A Compact UWB Koch Fractal Antenna for UWB Antenna Array Applications," *Wireless Personal Communications*, vol. 92, no. 4, pp. 1423-1442, Feb. 2017, <https://doi.org/10.1007/s11277-016-3613-1>.
- [27] S. S. Kadam, N. S. Patil, P. B. Jadhav, and P. B. Kashid, "Formation of Fractal Antenna Array for Multiband Applications," *International Journal of Recent Technology and Engineering*, vol. 8, no. 4, pp. 3257-3263, Nov. 2019, <https://doi.org/10.35940/ijrte.D8048.118419>.
- [28] R. A. Pandhare, P. L. Zade, and M. P. Abegaonkar, "Miniaturized microstrip antenna array using defected ground structure with enhanced performance," *Engineering Science and Technology, an International Journal*, vol. 19, no. 3, pp. 1360-1367, Sep. 2016, <https://doi.org/10.1016/j.jestech.2016.03.007>.
- [29] S. Palanisamy, B. Thangaraju, O. I. Khalaf, Y. Alotaibi, S. Alghamdi, and F. Alassery, "A Novel Approach of Design and Analysis of a Hexagonal Fractal Antenna Array (HFAA) for Next-Generation Wireless Communication," *Energies*, vol. 14, no. 19, Jan. 2021, Art. no. 6204, <https://doi.org/10.3390/en14196204>.
- [30] S. Nagaraju, B. V. Kadam, L. J. Gudino, S. M. Nagaraja, and N. Dave, "Performance analysis of rectangular, triangular and E-shaped microstrip patch antenna arrays for wireless sensor networks," in *International Conference on Computer and Communication Technology*, Allahabad, India, Sep. 2014, pp. 211-215, <https://doi.org/10.1109/ICCCT.2014.7001494>.